



LAWRENCE  
LIVERMORE  
NATIONAL  
LABORATORY

# Energy-Dependent Fission Q Values Generalized for All Actinides

R. Vogt

October 8, 2008

## **Disclaimer**

---

This document was prepared as an account of work sponsored by an agency of the United States government. Neither the United States government nor Lawrence Livermore National Security, LLC, nor any of their employees makes any warranty, expressed or implied, or assumes any legal liability or responsibility for the accuracy, completeness, or usefulness of any information, apparatus, product, or process disclosed, or represents that its use would not infringe privately owned rights. Reference herein to any specific commercial product, process, or service by trade name, trademark, manufacturer, or otherwise does not necessarily constitute or imply its endorsement, recommendation, or favoring by the United States government or Lawrence Livermore National Security, LLC. The views and opinions of authors expressed herein do not necessarily state or reflect those of the United States government or Lawrence Livermore National Security, LLC, and shall not be used for advertising or product endorsement purposes.

This work performed under the auspices of the U.S. Department of Energy by Lawrence Livermore National Laboratory under Contract DE-AC52-07NA27344.

# Energy-Dependent Fission $Q$ Values Generalized for All Actinides<sup>\*</sup>

R. Vogt

Lawrence Livermore National Laboratory  
P. O. Box 808  
Livermore, California 94551

We generalize Madland's parameterization of the energy release in fission to obtain the dependence of the fission  $Q$  values on incident neutron energy,  $E_n$ , for all major and minor actinides. These  $Q(E_n)$  parameterizations are included in the ENDL2008 release.

---

<sup>0\*</sup>This work was performed under the auspices of the U.S. Department of Energy by University of California, Lawrence Livermore National Laboratory under Contract DE-AC52-07NA27344. R.V. was supported in part by the National Science Foundation Grant NSF PHY-0555660.

This paper describes calculations of energy-dependent fission  $Q$  values based on parameterizations of the prompt energy release in fission [1], developed by Madland [1] to describe the prompt energy release in neutron-induced fission of  $^{235}\text{U}$ ,  $^{238}\text{U}$ , and  $^{239}\text{Pu}$ . The energy release is then related to the energy deposited during fission so that experimentally measurable quantities can be used to obtain the  $Q$  values. A discussion of these specific parameterizations and their implementation in the processing code for Monte Carlo neutron transport, **MCFG**EN, [2] is described in Ref. [3]. We extend this model to describe  $Q(E)$  for all actinides, major and minor, in the Evaluated Nuclear Data Library (ENDL) 2008 release, ENDL2008.

The ingredients of the deposited energy and thus the fission  $Q$  value are the average total fission product<sup>1</sup> kinetic energy,  $\langle T_p^{\text{tot}} \rangle$ , the average energy carried away by prompt emission of neutrons and gammas,  $\langle E_{\text{neut}}^{\text{tot}} \rangle$  and  $\langle E_{\gamma}^{\text{tot}} \rangle$  respectively, and the incident neutron energy  $E_n$ . On the event level, the incident neutron energy is known and the final state contributions are observables so that all the components could be measured. The average energy deposited by the fission event,  $\langle E_d \rangle$ , is [1]

$$\langle E_d(E_n) \rangle = \langle T_p^{\text{tot}}(E_n) \rangle + \langle E_{\text{neut}}^{\text{tot}}(E_n) \rangle + \langle E_{\gamma}^{\text{tot}}(E_n) \rangle . \quad (1)$$

The  $Q$  value then the difference between the deposited energy and the incident neutron energy,

$$Q(E_n) = \langle E_d \rangle - E_n . \quad (2)$$

Note that while energy would be conserved on the event level, Eqs. (1) and (2) only conserve energy on average.

The energy dependence of the contributions to  $\langle E_d \rangle$  can be fit to a polynomial form,

$$\langle E_i(E_n) \rangle = c_i + b_i E_n + a_i E_n^2 \quad (3)$$

where  $i$  is TKE,  $n$  and  $\gamma$  for  $E_i \equiv T_p^{\text{tot}}$ ,  $E_{\text{neut}}^{\text{tot}}$  and  $E_{\gamma}^{\text{tot}}$  respectively. Due to dimensional considerations, since  $E_n$  has units of MeV,  $a_i$  has units of  $\text{MeV}^{-1}$ ,  $b_i$  is dimensionless and  $c_i$  is in units of MeV. We do not consider any accuracy higher than a quadratic energy dependence.

In ENDL, each isotope is designated by its **ZA** value, **ZA** = 1000**Z** + **A**. There is a directory for each **ZA** combination [4]. In the directories, there are several descriptors used to specify the outgoing particle, **yo**: the reaction type (**C** numbers) and the reaction properties (**I** files) are most relevant for our discussion. Fission properties are found in files with **C**=15. We are primarily concerned with prompt neutron and gamma emission, **yo**=1 and 7 respectively. We neglect charged particle emission. The **I**=10 files contain

---

<sup>1</sup>The product kinetic energy is the kinetic energy of the fission fragments after prompt emission.

Isotope	Linear Fit		Quadratic Fit		
	$b_\gamma$	$c_\gamma$ (MeV)	$a_\gamma$ (MeV <sup>-1</sup> )	$b_\gamma$	$c_\gamma$ (MeV)
<sup>232</sup> U	0.01603	7.253	0.000182	0.0255	7.256
<sup>235</sup> U	0.1398	7.359	-0.00474	0.2295	7.284
<sup>238</sup> U	0.01606	6.658	$-1.22 \times 10^{-7}$	0.01607	6.658
<sup>239</sup> Pu	0.2379	7.014	-0.009878	0.4249	6.857
<sup>252</sup> Cf	0.01831	6.44186	-	-	-
generic	0.01693	6.949	$7.238 \times 10^{-8}$	0.01693	6.95

Table 1: Coefficients of linear and quadratic fits to the average outgoing prompt gamma energy as a function of incident neutron energy. The individual slope and intercept are given for the isotopes where additional values are available. For those isotopes where the information is unknown, a generic energy dependence is given.

the average energy deposited to light ejectiles. We make fits to the I=10 files to obtain the energy dependence of  $\langle E_{\text{neut}}^{\text{tot}} \rangle$  and  $\langle E_\gamma^{\text{tot}} \rangle$ .

We begin with the energy deposited in gammas since this information is rather sparse. The I=10 files for gammas are typically generic and are almost independent of incident energy. The fit coefficients for  $i = \gamma$  in Eq. (3) are given in Table 1. Note that not every actinide isotope has a corresponding I=10 file for prompt gamma emission. Some of those that do exhibit somewhat unphysical behavior. The fit values designated <sup>232</sup>U in Table 1 are also used for <sup>233</sup>U, <sup>234</sup>U, <sup>236</sup>U, <sup>237</sup>U, <sup>240</sup>U and <sup>241</sup>U since they all have the same I=10 files. The <sup>235</sup>U, <sup>239</sup>Pu and <sup>252</sup>Cf I=10 files in ENDL2008 all exhibit unphysical cutoffs above about 1 MeV, after which the energy in prompt photon emission drops to zero. For these isotopes, we have substituted the ENDL99 I=10 files in the fits. In the cases where the gamma I=10 files are missing, we have substituted the generic case, obtained from the <sup>239</sup>U fit. We have made both linear and quadratic fits when possible. However, since the gamma I=10 files typically contain only 2 or 3 energy points ( $10^{-10}$ ,  $[14]^2$  and 20 MeV), we use the linear fits in the calculation of  $Q(E_n)$ . Note that, except for <sup>235</sup>U and <sup>239</sup>Pu, the coefficients of the quadratic term,  $a_\gamma$ , are small and the parameters  $b_\gamma$  and  $c_\gamma$  do not depend strongly on whether the fit is linear or quadratic. We thus do not provide uncertainties on the fit parameters.

The resulting energy dependence of  $\langle E_\gamma^{\text{tot}} \rangle$  is shown in Fig. 1. Only <sup>235</sup>U and <sup>239</sup>Pu show a significant energy dependence. Since there are so few data available, it is not clear how generic the ‘generic’ dependence actually is. One might naively expect that more energy is taken away by gamma emission as the actinide  $A$  and the incident neutron energy increase. However, prompt gamma emission comes only after the fission product excitation energy drops below the neutron separation energy of a few MeV. Therefore the fragment

---

<sup>2</sup>We put  $E_n = 14$  MeV in brackets because it is the value excluded from the I=10 file for <sup>252</sup>Cf with two energy points.

is at a similar level of excitation when prompt gamma emission begins, regardless of the incident neutron energy. Consequently, the separation energy should thus provide a lower bound on  $\langle E_\gamma^{\text{tot}} \rangle$ , independent of  $E_n$ , and its dependence on incident energy may indeed be slow. A stronger variation with  $A$  may, however, be expected since the neutron separation energy depends on the individual fragment pairing energy.

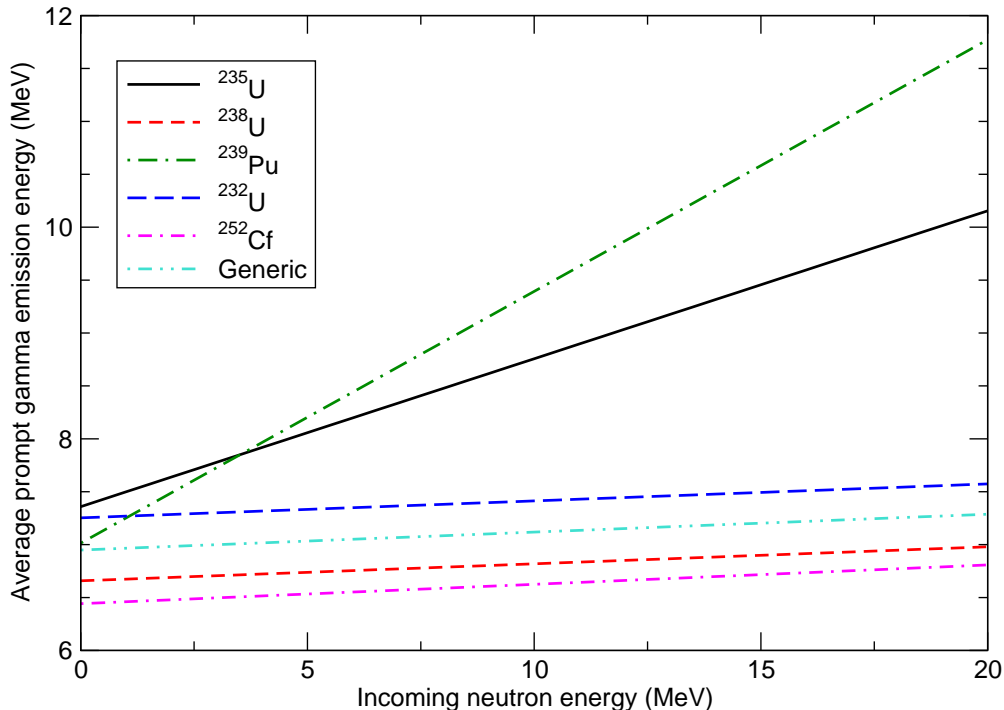


Figure 1: The model average prompt gamma emission energy for the isotopes listed in Table 1.

There are neutron  $I=10$  files for all the actinides in ENDL2008. These files typically contain 20–30 or more points, making good quadratic fits possible<sup>3</sup>. We compare the linear and quadratic fit coefficients and their uncertainties for  $E_i \equiv E_{\text{neut}}^{\text{tot}}$  in Eq. (3) in Tables 2–11. The fluctuations in  $c_n$  can in part be explained by the pairing terms. Even-even and odd-odd  $Z, N$  combinations are more strongly bound than even-odd and odd-even nuclei. Thus more energy would be required to evaporate a neutron and the energy of neutrons

<sup>3</sup>A notable exception is  $^{244}\text{Am}$  with only three points at  $10^{-11}$ ,  $2.53 \times 10^{-8}$  and 20 MeV. We note also that while Am has two pairs of isomeric states ( $^{242}\text{Am}$  and  $^{242\text{m}}\text{Am}$  as well as  $^{244}\text{Am}$  and  $^{244\text{m}}\text{Am}$ ) the neutron  $I=10$  files in ENDL2008 are the same for the two states of each pair, *e.g.* they are identical for  $^{242}\text{Am}$  and  $^{242\text{m}}\text{Am}$ .

Actinium ( $_{89}\text{Ac}$ )				
Isotope	Linear Fit			
	$b_n$	$c_n$ (MeV)	$L^2/\text{dof}$	
225	$0.1697 \pm 0.0035$	$3.532 \pm 0.035$	0.428/29	
226	$0.2041 \pm 0.0064$	$3.451 \pm 0.063$	1.416/29	
227	$0.1862 \pm 0.0042$	$3.402 \pm 0.041$	0.609/29	

Isotope	Quadratic Fit			
	$a_n$ ( $\text{MeV}^{-1}$ )	$b_n$	$c_n$ (MeV)	$L^2/\text{dof}$
225	$-0.001317 \pm 0.000633$	$0.1937 \pm 0.0120$	$3.478 \pm 0.042$	0.369/28
226	$0.004442 \pm 0.000897$	$0.1231 \pm 0.0170$	$3.635 \pm 0.060$	0.742/28
227	$-0.000144 \pm 0.000812$	$0.1888 \pm 0.0154$	$3.396 \pm 0.054$	0.608/28

Table 2: Coefficients of linear and quadratic fits to the average outgoing prompt neutron energy as a function of incident neutron energy for the Actinium isotopes ( $Z = 89$ ).

emitted from even-even and odd-odd mother nuclei should be lower than from even-odd and odd-even mother isotopes. This is generally the case in the neutron I=10 fits, as can be seen by examination of Tables 2-11.

The fits to the I=10 files were done using the CERN ROOT software package which gives both the best fit and the fit parameter uncertainty. Since there are no error bars on the evaluated data in the I=10 files, the goodness of fit,  $L^2$ , is obtained by minimizing the difference between the files and Eq. (3). We also give the  $L^2$  per degree of freedom for both fits. The linear fits often have  $L^2 > 1$  while  $L^2$  is generally smaller and, in many cases, less than one for the quadratic fits. Since the quadratic approximation gives a better fit, it is used in the calculation of  $Q(E_n)$ .

An example of the fits to  $\langle E_{\text{neut}}^{\text{tot}}(E_n) \rangle$  are shown in Fig. 2 for  $^{235}\text{U}$ ,  $^{238}\text{U}$  and  $^{239}\text{Pu}$ . The dashed lines are the linear fits while the solid curves show the quadratic fits. The ENDL2008 points exhibit some fluctuation inconsistent with both a linear and a quadratic fit. These fluctuations occur at the thresholds for multiple chance fission. The average fission neutron kinetic energy is related to the product of the average energy per neutron and the average neutron multiplicity per fission [1]. The average energy per neutron is small, on the order of 1 MeV or so, and increases slowly with  $E_n$ . The fluctuations due to multichance fission are in this component. The neutron multiplicity increases nearly linearly with  $E_n$ , causing the observed increase in the I=10 files.

We model the average fission product kinetic energy based on rather simple assumptions. A Coulomb approximation of the total fission kinetic energy for thermal neutrons ( $E_n \approx 0$ ) is

$$\langle T_p^{\text{tot}}(E_n = 0) \rangle = \alpha \hbar c \frac{Z_L Z_H}{R_{AL} + R_{AH} + d_{LH}} , \quad (4)$$

*e.g.* the total fragment kinetic energy is directly proportional to the product

Thorium ( $_{90}\text{Th}$ )				
Isotope	Linear Fit			
	$b_n$	$c_n$ (MeV)	$L^2/\text{dof}$	
227	$0.2423 \pm 0.0081$	$4.003 \pm 0.078$	2.345/30	
228	$0.2806 \pm 0.0043$	$3.646 \pm 0.041$	0.731/32	
229	$0.2482 \pm 0.0080$	$3.957 \pm 0.077$	2.296/30	
230	$0.2762 \pm 0.0098$	$3.544 \pm 0.092$	3.836/32	
231	$0.2366 \pm 0.0095$	$3.819 \pm 0.093$	3.769/33	
232	$0.3372 \pm 0.0216$	$3.432 \pm 0.245$	0.196/3	
233	$0.2683 \pm 0.0093$	$3.714 \pm 0.095$	0.206/7	
234	$0.2924 \pm 0.0084$	$3.244 \pm 0.081$	2.514/30	

Isotope	Quadratic Fit			
	$a_n$ ( $\text{MeV}^{-1}$ )	$b_n$	$c_n$ (MeV)	$L^2/\text{dof}$
227	$0.006569 \pm 0.000955$	$0.1225 \pm 0.0181$	$4.275 \pm 0.062$	0.871/29
228	$0.003449 \pm 0.000526$	$0.2181 \pm 0.0099$	$3.787 \pm 0.034$	0.3/31
229	$0.006267 \pm 0.001000$	$0.1339 \pm 0.0190$	$4.216 \pm 0.065$	0.955/29
230	$0.007380 \pm 0.001324$	$0.1422 \pm 0.0250$	$3.847 \pm 0.086$	1.885/31
231	$0.006487 \pm 0.001383$	$0.1196 \pm 0.0260$	$4.095 \pm 0.093$	2.205/32
232	$-0.000431 \pm 0.005136$	$0.3465 \pm 0.1152$	$3.401 \pm 0.509$	0.194/2
233	$0.000663 \pm 0.001607$	$0.2566 \pm 0.0300$	$3.736 \pm 0.115$	0.2/6
234	$0.003476 \pm 0.001483$	$0.2290 \pm 0.0281$	$3.387 \pm 0.097$	2.102/29

Table 3: Coefficients of linear and quadratic fits to the average outgoing prompt neutron energy as a function of incident neutron energy for the Thorium isotopes ( $Z = 90$ ).

Protactinium ( $_{91}\text{Pa}$ )				
Isotope	Linear Fit			
	$b_n$	$c_n$ (MeV)	$L^2/\text{dof}$	
229	$0.2735 \pm 0.0070$	$4.381 \pm 0.068$	1.766/30	
230	$0.2893 \pm 0.0066$	$4.490 \pm 0.063$	1.549/30	
231	$0.2900 \pm 0.0090$	$4.258 \pm 0.087$	2.920/30	
232	$0.2916 \pm 0.0090$	$4.419 \pm 0.087$	2.947/30	
233	$0.3800 \pm 0.0135$	$4.035 \pm 0.160$	0.185/5	

Isotope	Quadratic Fit			
	$a_n$ ( $\text{MeV}^{-1}$ )	$b_n$	$c_n$ (MeV)	$L^2/\text{dof}$
229	$0.005433 \pm 0.000890$	$0.1744 \pm 0.0169$	$4.605 \pm 0.058$	0.758/29
230	$0.005562 \pm 0.000718$	$0.1879 \pm 0.0136$	$4.720 \pm 0.047$	0.493/29
231	$0.006436 \pm 0.001255$	$0.1726 \pm 0.0238$	$4.524 \pm 0.082$	1.506/29
232	$0.006763 \pm 0.001204$	$0.1683 \pm 0.0228$	$4.699 \pm 0.079$	1.386/29
233	$0.000639 \pm 0.002447$	$0.3671 \pm 0.0516$	$4.076 \pm 0.242$	0.181/4

Table 4: Coefficients of linear and quadratic fits to the average outgoing prompt neutron energy as a function of incident neutron energy for the Protactinium isotopes ( $Z = 91$ ).



Uranium ( $_{92}\text{U}$ )				
Isotope	Linear Fit			
	$b_n$	$c_n$ (MeV)	$L^2/\text{dof}$	
230	$0.3070 \pm 0.0072$	$4.696 \pm 0.070$	1.89/30	
231	$0.3186 \pm 0.0062$	$4.956 \pm 0.060$	1.41/30	
232	$0.3383 \pm 0.0066$	$6.051 \pm 0.052$	0.082/6	
233	$0.3066 \pm 0.0066$	$5.040 \pm 0.061$	0.370/14	
234	$0.2868 \pm 0.0065$	$4.571 \pm 0.074$	0.654/20	
235	$0.2877 \pm 0.0033$	$4.903 \pm 0.029$	0.36/29	
236	$0.3694 \pm 0.0096$	$4.423 \pm 0.090$	0.0726/4	
237	$0.3002 \pm 0.0048$	$4.923 \pm 0.048$	0.528/24	
238	$0.2757 \pm 0.0077$	$4.713 \pm 0.082$	1.692/26	
239	$0.4472 \pm 0.0129$	$4.409 \pm 0.150$	0.160/4	
240	$0.3648 \pm 0.0138$	$4.553 \pm 0.157$	0.316/5	
241	$0.4513 \pm 0.0059$	$4.184 \pm 0.053$	0.107/8	

Isotope	Quadratic Fit			
	$a_n$ ( $\text{MeV}^{-1}$ )	$b_n$	$c_n$ (MeV)	$L^2/\text{dof}$
230	$0.006792 \pm 0.000575$	$0.1832 \pm 0.0109$	$4.977 \pm 0.038$	0.316/29
231	$0.005808 \pm 0.000518$	$0.2127 \pm 0.0098$	$5.196 \pm 0.034$	0.256/29
232	$0.003243 \pm 0.000167$	$0.2782 \pm 0.0032$	$6.082 \pm 0.006$	0.00086/5
233	$0.002915 \pm 0.000873$	$0.2540 \pm 0.0165$	$5.141 \pm 0.055$	0.1919/13
234	$0.002704 \pm 0.000988$	$0.2339 \pm 0.0201$	$4.728 \pm 0.086$	0.462/19
235	$-0.001424 \pm 0.000572$	$0.3114 \pm 0.0100$	$4.864 \pm 0.031$	0.2925/28
236	$0.004555 \pm 0.001122$	$0.2969 \pm 0.0182$	$4.505 \pm 0.042$	0.00785/3
237	$0.001783 \pm 0.000811$	$0.2680 \pm 0.0153$	$4.999 \pm 0.057$	0.433/23
238	$-0.004351 \pm 0.001295$	$0.3574 \pm 0.0252$	$4.509 \pm 0.092$	1.151/25
239	$0.004266 \pm 0.000007$	$0.3647 \pm 0.0001$	$4.580 \pm 0.0005$	$8.16 \times 10^{-7}/3$
240	$0.000273 \pm 0.003723$	$0.3596 \pm 0.0721$	$4.561 \pm 0.211$	0.315/4
241	$0.002821 \pm 0.000050$	$0.3998 \pm 0.0010$	$4.268 \pm 0.003$	0.000201/7

Table 5: Coefficients of linear and quadratic fits to the average outgoing prompt neutron energy as a function of incident neutron energy for the Uranium isotopes ( $Z = 92$ ).

Neptunium ( $_{93}\text{Np}$ )				
Isotope	Linear Fit			
	$b_n$	$c_n$ (MeV)	$L^2/\text{dof}$	
234	$0.3704 \pm 0.0084$	$5.565 \pm 0.081$	2.518/30	
235	$0.3898 \pm 0.0082$	$5.256 \pm 0.079$	2.429/30	
236	$0.3927 \pm 0.0087$	$4.744 \pm 0.084$	2.739/30	
237	$0.3710 \pm 0.0031$	$5.250 \pm 0.022$	3.942/107	
238	$0.4028 \pm 0.0085$	$4.901 \pm 0.082$	2.626/30	
239	$0.3215 \pm 0.0050$	$5.302 \pm 0.044$	1.787/41	

Isotope	Quadratic Fit			
	$a_n$ ( $\text{MeV}^{-1}$ )	$b_n$	$c_n$ (MeV)	$L^2/\text{dof}$
234	$0.007642 \pm 0.000741$	$0.2311 \pm 0.0141$	$5.880 \pm 0.048$	0.524/29
235	$0.007751 \pm 0.000629$	$0.2484 \pm 0.0119$	$5.576 \pm 0.041$	0.378/29
236	$0.008116 \pm 0.000716$	$0.2446 \pm 0.0136$	$5.080 \pm 0.047$	0.490/29
237	$0.005819 \pm 0.000404$	$0.2768 \pm 0.0068$	$5.330 \pm 0.014$	1.325/106
238	$0.007559 \pm 0.000841$	$0.2650 \pm 0.0160$	$5.214 \pm 0.055$	0.676/29
239	$0.004159 \pm 0.000767$	$0.2489 \pm 0.0139$	$5.416 \pm 0.040$	1.019/40

Table 6: Coefficients of linear and quadratic fits to the average outgoing prompt neutron energy as a function of incident neutron energy for the Neptunium isotopes ( $Z = 93$ ).

of the fragment charges and inversely proportional to the separation of the fragment centers at scission. We take  $d_{LH} = 1.5$  fm and  $R_A = r_0 A^{1/3}(1 + 2\beta_1/3)$  with  $r_0 = 1.16$  fm and  $\beta_1 = 0.625$  [5]. For actinides up to Cm, we assume that, on average, the heavy fragment has  $A_H = 140$ . Above  $Z = 96$ , we increment the average  $A$  by 1. The charge of the heavy fragment is obtained assuming  $Z_H = A_H(Z/A) - 1/2$ . The mass and charge of the light fragment is obtained by energy conservation:  $A_L = A - A_H$  and  $Z_L = Z - Z_H$ . The small variations in  $c_{\text{TKE}}$  for a given actinide  $\text{ZA}$  is primarily due to the relative  $Z_L$  and  $Z_H$  of the fission products since  $R_{A_L} + R_{A_H} \approx R_A$ .

Madland observed that the average fission product kinetic energy decreases with  $E_n$ . We note that the slope seems to be a slowly increasing function of  $Z$  [1]. The  $Z$  dependence of the slope,  $b_{\text{TKE}}$ , is based on the difference between the  $^{239}\text{Pu}$  slope and the average of the  $^{235}\text{U}$  and  $^{238}\text{U}$  slopes in Ref. [1]. Thus the lighter actinides have a slower decrease in kinetic energy with  $E_n$  than the heavier ones. We do not attempt to model more than a linear approximation to the fission product kinetic energy. The coefficients we obtain for  $i = \text{TKE}$  are given in Tables 12-21.

Plutonium ( $_{94}\text{Pu}$ )				
Isotope	Linear Fit			
	$b_n$	$c_n$ (MeV)	$L^2/\text{dof}$	
236	$0.3876 \pm 0.0104$	$5.751 \pm 0.096$	3.355/29	
237	$0.3837 \pm 0.0070$	$5.897 \pm 0.068$	1.769/30	
238	$0.3637 \pm 0.0099$	$5.768 \pm 0.091$	3.009/29	
239	$0.3275 \pm 0.0048$	$6.191 \pm 0.044$	0.495/25	
240	$0.3995 \pm 0.0101$	$5.572 \pm 0.093$	3.138/29	
241	$0.3998 \pm 0.0105$	$5.800 \pm 0.096$	3.390/29	
242	$0.3665 \pm 0.0101$	$5.601 \pm 0.093$	3.131/29	
243	$0.5813 \pm 0.0140$	$5.549 \pm 0.177$	0.300/5	
244	$0.4110 \pm 0.0106$	$5.313 \pm 0.098$	3.468/29	
246	$0.4599 \pm 0.0100$	$4.818 \pm 0.097$	3.638/30	

Isotope	Quadratic Fit			
	$a_n$ ( $\text{MeV}^{-1}$ )	$b_n$	$c_n$ (MeV)	$L^2/\text{dof}$
236	$0.009279 \pm 0.000939$	$0.2240 \pm 0.0173$	$6.112 \pm 0.017$	0.727/28
237	$0.006790 \pm 0.000452$	$0.2599 \pm 0.0086$	$6.177 \pm 0.030$	0.196/29
238	$0.008211 \pm 0.001074$	$0.2189 \pm 0.0198$	$6.087 \pm 0.067$	0.951/28
239	$-0.002495 \pm 0.000736$	$0.3707 \pm 0.0134$	$6.092 \pm 0.047$	0.331/24
240	$0.008608 \pm 0.001031$	$0.2477 \pm 0.0190$	$5.906 \pm 0.064$	0.877/28
241	$0.009310 \pm 0.000950$	$0.2356 \pm 0.0175$	$6.161 \pm 0.059$	0.744/28
242	$0.008356 \pm 0.001102$	$0.2192 \pm 0.0203$	$5.926 \pm 0.068$	1/28
243	$0.005751 \pm 0.000536$	$0.4692 \pm 0.0108$	$5.781 \pm 0.039$	0.00764/4
244	$0.008807 \pm 0.001156$	$0.2557 \pm 0.0213$	$5.655 \pm 0.072$	1.1/28
246	$0.007922 \pm 0.001251$	$0.3155 \pm 0.0237$	$5.145 \pm 0.082$	1.5/29

Table 7: Coefficients of linear and quadratic fits to the average outgoing prompt neutron energy as a function of incident neutron energy for the Plutonium isotopes ( $Z = 94$ ).

Americium ( $_{95}\text{Am}$ )				
Isotope	Linear Fit			
	$b_n$	$c_n$ (MeV)	$L^2/\text{dof}$	
240	$0.3891 \pm 0.0059$	$7.054 \pm 0.060$	0.334/15	
241	$0.3348 \pm 0.0060$	$7.227 \pm 0.070$	2.033/38	
242	$0.3891 \pm 0.0059$	$7.054 \pm 0.060$	0.334/15	
243	$0.3059 \pm 0.0049$	$7.562 \pm 0.055$	1.329/39	
244	$0.3837 \pm 0.0612$	$6.543 \pm 0.707$	0/1	

Isotope	Quadratic Fit			
	$a_n$ ( $\text{MeV}^{-1}$ )	$b_n$	$c_n$ (MeV)	$L^2/\text{dof}$
240	$0.002294 \pm 0.000895$	$0.3473 \pm 0.0171$	$7.150 \pm 0.063$	0.222/14
241	$-0.004504 \pm 0.000817$	$0.4243 \pm 0.0168$	$6.957 \pm 0.071$	1.102/37
242	$0.002294 \pm 0.000895$	$0.3473 \pm 0.0171$	$7.150 \pm 0.063$	0.222/14
243	$-0.002387 \pm 0.000824$	$0.3523 \pm 0.0166$	$7.422 \pm 0.070$	1.083/38

Table 8: Coefficients of linear and quadratic fits to the average outgoing prompt neutron energy as a function of incident neutron energy for the Americium isotopes ( $Z = 95$ ). Note that the  $^{240}\text{Am}$  neutron energy spectra have been taken over from  $^{242}\text{Am}$ . Since there are not enough points in the  $^{244}\text{Am}$  I=10 file for a meaningful quadratic fit, no values are given above.

Curium ( $_{96}\text{Cm}$ )				
Isotope	Linear Fit			
	$b_n$	$c_n$ (MeV)	$L^2/\text{dof}$	
240	$0.4800 \pm 0.0118$	$7.069 \pm 0.114$	4.996/30	
241	$0.4983 \pm 0.0078$	$7.397 \pm 0.076$	2.217/30	
242	$0.4884 \pm 0.0177$	$7.087 \pm 0.202$	5.148/20	
243	$0.3389 \pm 0.0116$	$7.827 \pm 0.127$	1.873/19	
244	$0.4084 \pm 0.0174$	$6.556 \pm 0.191$	4.23/19	
245	$0.3268 \pm 0.0106$	$7.743 \pm 0.113$	1.81/20	
246	$0.4000 \pm 0.0158$	$6.465 \pm 0.173$	3.466/19	
247	$0.5412 \pm 0.0101$	$7.882 \pm 0.093$	3.137/29	
248	$0.5031 \pm 0.0224$	$6.611 \pm 0.245$	6.964/19	
249	$0.5402 \pm 0.0107$	$6.756 \pm 0.104$	4.141/30	
250	$0.5267 \pm 0.0094$	$6.707 \pm 0.087$	2.758/29	

Isotope	Quadratic Fit			
	$a_n$ ( $\text{MeV}^{-1}$ )	$b_n$	$c_n$ (MeV)	$L^2/\text{dof}$
240	$0.011040 \pm 0.000933$	$0.2786 \pm 0.0177$	$7.525 \pm 0.061$	0.833/29
241	$0.007316 \pm 0.000638$	$0.3648 \pm 0.0121$	$7.699 \pm 0.042$	0.390/29
242	$0.011400 \pm 0.001962$	$0.2683 \pm 0.0394$	$7.701 \pm 0.162$	1.791/19
243	$0.005492 \pm 0.001729$	$0.2363 \pm 0.0337$	$8.104 \pm 0.135$	1.176/18
244	$0.010830 \pm 0.001966$	$0.2061 \pm 0.0383$	$7.103 \pm 0.154$	1.52/18
245	$0.005426 \pm 0.001550$	$0.2279 \pm 0.0295$	$7.984 \pm 0.113$	1.08/19
246	$0.009390 \pm 0.001995$	$0.2245 \pm 0.0371$	$6.939 \pm 0.149$	1.43/18
247	$0.008595 \pm 0.001035$	$0.3896 \pm 0.0190$	$8.216 \pm 0.064$	0.882/28
248	$0.013550 \pm 0.002629$	$0.2499 \pm 0.0512$	$7.295 \pm 0.206$	2.717/18
249	$0.008907 \pm 0.001224$	$0.3777 \pm 0.0232$	$7.124 \pm 0.080$	1.432/29
250	$0.006831 \pm 0.001272$	$0.4062 \pm 0.0234$	$6.973 \pm 0.079$	1.334/28

Table 9: Coefficients of linear and quadratic fits to the average outgoing prompt neutron energy as a function of incident neutron energy for the Curium isotopes ( $Z = 96$ ).

Berkelium ( $_{97}\text{Bk}$ )				
Isotope	Linear Fit			
	$b_n$	$c_n$ (MeV)	$L^2/\text{dof}$	
245	$0.5396 \pm 0.0110$	$7.801 \pm 0.105$	4.47/31	
246	$0.5757 \pm 0.0057$	$8.042 \pm 0.054$	1.2/31	
247	$0.5749 \pm 0.0087$	$7.495 \pm 0.084$	2.76/30	
248	$0.6010 \pm 0.0070$	$7.862 \pm 0.067$	1.82/31	
249	$0.5868 \pm 0.0111$	$7.100 \pm 0.107$	4.45/30	
250	$0.5719 \pm 0.0103$	$7.536 \pm 0.100$	3.84/30	

Isotope	Quadratic Fit			
	$a_n$ ( $\text{MeV}^{-1}$ )	$b_n$	$c_n$ (MeV)	$L^2/\text{dof}$
245	$0.009615 \pm 0.001067$	$0.3643 \pm 0.0203$	$8.210 \pm 0.071$	1.176/30
246	$0.005445 \pm 0.000371$	$0.4764 \pm 0.0071$	$8.274 \pm 0.025$	0.142/30
247	$0.008129 \pm 0.000723$	$0.4266 \pm 0.0137$	$7.831 \pm 0.047$	0.499/29
248	$0.006656 \pm 0.000481$	$0.4796 \pm 0.0091$	$8.145 \pm 0.032$	0.239/30
249	$0.010130 \pm 0.000996$	$0.4021 \pm 0.0189$	$7.519 \pm 0.065$	0.948/29
250	$0.008308 \pm 0.001245$	$0.4204 \pm 0.0236$	$7.879 \pm 0.081$	1.482/29

Table 10: Coefficients of linear and quadratic fits to the average outgoing prompt neutron energy as a function of incident neutron energy for the Berkelium isotopes ( $Z = 97$ ).

Californium ( $_{98}\text{Cf}$ )				
Isotope	Linear Fit			
	$b_n$	$c_n$ (MeV)	$L^2/\text{dof}$	
246	$0.5964 \pm 0.0094$	$8.518 \pm 0.090$	3.3/31	
248	$0.5829 \pm 0.0120$	$8.207 \pm 0.116$	5.41/31	
249	$0.6035 \pm 0.0081$	$9.136 \pm 0.078$	2.36/30	
250	$0.6329 \pm 0.0076$	$7.921 \pm 0.074$	2.10/30	
251	$0.6423 \pm 0.0121$	$8.961 \pm 0.117$	5.25/30	
252	$0.6501 \pm 0.0074$	$8.330 \pm 0.071$	1.96/30	
253	$0.5796 \pm 0.0198$	$7.657 \pm 0.190$	14.65/31	

Isotooe	Quadratic Fit			
	$a_n$ ( $\text{MeV}^{-1}$ )	$b_n$	$c_n$ (MeV)	$L^2/\text{dof}$
246	$0.009000 \pm 0.000633$	$0.4323 \pm 0.0120$	$8.900 \pm 0.042$	0.414/30
248	$0.010700 \pm 0.001134$	$0.3877 \pm 0.0216$	$8.661 \pm 0.076$	1.33/30
249	$0.007067 \pm 0.000826$	$0.4746 \pm 0.0157$	$9.428 \pm 0.054$	0.653/29
250	$0.007397 \pm 0.000492$	$0.4980 \pm 0.0093$	$8.226 \pm 0.032$	0.232/29
251	$0.010790 \pm 0.001153$	$0.4454 \pm 0.0219$	$9.407 \pm 0.075$	1.27/29
252	$0.007184 \pm 0.000455$	$0.5190 \pm 0.0086$	$8.627 \pm 0.030$	0.198/29
253	$0.018650 \pm 0.001478$	$0.2396 \pm 0.0281$	$8.449 \pm 0.098$	2.26/30

Table 11: Coefficients of linear and quadratic fits to the average outgoing prompt neutron energy as a function of incident neutron energy for the Californium isotopes ( $Z = 98$ ).

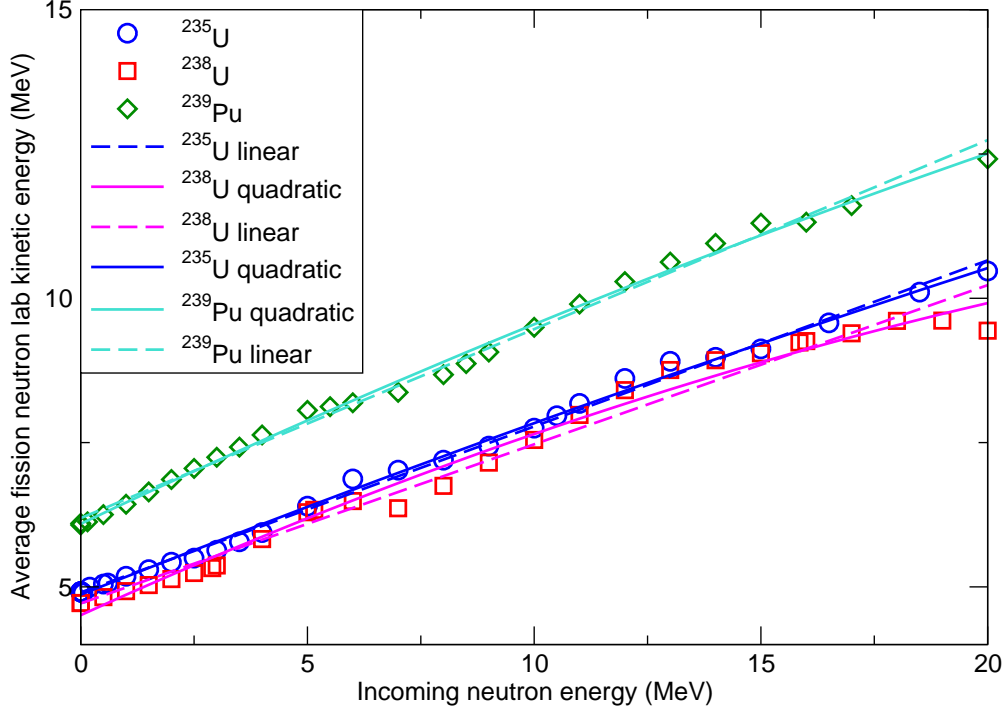


Figure 2: The fitted average prompt neutron energy in the lab frame for the linear (dashed) and quadratic (solid) fits for  $^{235}\text{U}$  (blue circles and curves),  $^{238}\text{U}$  (red squares, magenta curves) and  $^{239}\text{Pu}$  (green diamonds, turquoise curves).

Actinium ( $_{89}\text{Ac}$ )					
Isotope	Product Kinetic Energy		$Q(E_n)$		
	$b_{\text{TKE}}$	$c_{\text{TKE}}$ (MeV)	$a_Q$ ( $\text{MeV}^{-1}$ )	$b_Q$	$c_Q$ (MeV)
225	-0.081996	157.989227	-0.001317	-0.871366	168.416227
226	-0.081863	157.731317	0.004442	-0.941833	168.315317
227	-0.081730	157.476229	-0.000144	-0.876000	167.821229

Table 12: Coefficients of a linear parameterization of the product kinetic energy and the quadratic coefficients of the  $Q(E_n)$  parameterization for the Actinium isotopes ( $Z = 89$ ).

Thorium ( $_{90}\text{Th}$ )					
Isotope	Product Kinetic Energy		$Q(E_n)$		
	$b_{\text{TKE}}$	$c_{\text{TKE}}$ (MeV)	$a_Q$ (MeV $^{-1}$ )	$b_Q$	$c_Q$ (MeV)
227	-0.150127	160.392455	0.006569	-1.010697	171.616455
228	-0.151366	161.716014	0.003449	-0.916336	172.452014
229	-0.151126	161.459258	0.006267	-1.000296	172.624258
230	-0.150888	161.205224	0.007380	-0.991758	172.001224
231	-0.150653	160.953853	0.006487	-1.014123	171.997853
232	-0.151735	162.110434	-0.000431	-0.788305	172.460434
233	-0.151503	161.862076	0.000663	-0.877973	172.547076
234	-0.151273	161.616242	0.003476	-0.905343	171.952242

Table 13: Coefficients of a linear parameterization of the product kinetic energy and the quadratic coefficients of the  $Q(E_n)$  parameterization for the Thorium isotopes ( $Z = 90$ ).

Protactinium ( $_{91}\text{Pa}$ )					
Isotope	Product Kinetic Energy		$Q(E_n)$		
	$b_{\text{TKE}}$	$c_{\text{TKE}}$ (MeV)	$a_Q$ (MeV $^{-1}$ )	$b_Q$	$c_Q$ (MeV)
229	-0.222500	164.449245	0.005433	-1.031170	176.003245
230	-0.224169	165.683147	0.005562	-1.019339	177.352146
231	-0.223820	165.424793	0.006436	-1.034290	176.897794
232	-0.223474	165.169122	0.006763	-1.038244	176.817122
233	-0.223131	164.916077	0.000639	-0.839101	175.941077

Table 14: Coefficients of a linear parameterization of the product kinetic energy and the quadratic coefficients of the  $Q(E_n)$  parameterization for the Protactinium isotopes ( $Z = 91$ ).



Uranium ( $_{92}\text{U}$ )					
Isotope	Product Kinetic Energy		$Q(E_n)$		
	$b_{\text{TKE}}$	$c_{\text{TKE}}$ (MeV)	$a_Q$ ( $\text{MeV}^{-1}$ )	$b_Q$	$c_Q$ (MeV)
230	-0.298690	168.751353	0.006792	-1.098560	180.677353
231	-0.298224	168.488216	0.005808	-1.068594	180.633216
232	-0.297763	168.227809	0.003425	-1.003533	181.562809
233	-0.299791	169.373268	0.002915	-1.029761	181.463268
234	-0.299335	169.116027	0.002704	-1.049405	180.793027
235	-0.298885	168.861376	-0.006164	-0.847685	181.084376
236	-0.298438	168.609264	0.004555	-0.985508	180.063264
237	-0.300175	169.590339	0.001783	-1.016145	181.538339
238	-0.299734	169.341348	-0.004351	-0.926264	180.508348
239	-0.299298	169.094769	0.004266	-0.917668	180.623768
240	-0.298865	168.850554	0.000273	-0.923235	180.360553
241	-0.300314	169.669091	0.002821	-0.884484	180.886091

Table 15: Coefficients of a linear parameterization of the product kinetic energy and the quadratic coefficients of the  $Q(E_n)$  parameterization for the Uranium isotopes ( $Z = 92$ ).

Neptunium ( $_{93}\text{Np}$ )					
Isotope	Product Kinetic Energy		$Q(E_n)$		
	$b_{\text{TKE}}$	$c_{\text{TKE}}$ (MeV)	$a_Q$ ( $\text{MeV}^{-1}$ )	$b_Q$	$c_Q$ (MeV)
234	-0.376706	172.247805	0.007642	-1.128676	185.076806
235	-0.379018	173.305096	0.007751	-1.113688	185.830097
236	-0.378452	173.046349	0.008116	-1.116922	185.075349
237	-0.377892	172.790156	0.005819	-1.084162	185.069156
238	-0.377337	172.536468	0.007559	-1.095407	184.699468
239	-0.379293	173.430532	0.004159	-1.113463	185.795532

Table 16: Coefficients of a linear parameterization of the product kinetic energy and the quadratic coefficients of the  $Q(E_n)$  parameterization for the Neptunium isotopes ( $Z = 93$ ).

Plutonium ( $_{94}\text{Pu}$ )					
Isotope	Product Kinetic Energy		$Q(E_n)$		
	$b_{\text{TKE}}$	$c_{\text{TKE}}$ (MeV)	$a_Q$ (MeV $^{-1}$ )	$b_Q$	$c_Q$ (MeV)
236	-0.458957	176.250911	0.009279	-1.218027	189.311911
237	-0.458278	175.989974	0.006790	-1.181448	189.115974
238	-0.460805	176.960480	0.008211	-1.224975	189.996480
239	-0.460134	176.702806	-0.012373	-0.851534	189.808806
240	-0.459470	176.447603	0.008608	-1.194840	189.302603
241	-0.458811	176.194825	0.009310	-1.206281	189.304825
242	-0.460917	177.003350	0.008356	-1.224787	189.878350
243	-0.460267	176.753793	0.005751	-0.974137	189.483793
244	-0.459623	176.506542	0.008807	-1.186993	189.110542
246	-0.460673	176.909821	0.007922	-1.128243	189.003821

Table 17: Coefficients of a linear parameterization of the product kinetic energy and the quadratic coefficients of the  $Q(E_n)$  parameterization for the Plutonium isotopes ( $Z = 94$ ).

Americium ( $_{95}\text{Am}$ )					
Isotope	Product Kinetic Energy		$Q(E_n)$		
	$b_{\text{TKE}}$	$c_{\text{TKE}}$ (MeV)	$a_Q$ (MeV $^{-1}$ )	$b_Q$	$c_Q$ (MeV)
240	-0.546374	180.858793	0.002294	-1.182144	194.957793
241	-0.545592	180.599695	-0.004504	-1.104362	194.505695
242	-0.544816	180.343036	0.002294	-1.180586	194.442036
243	-0.544048	180.088770	-0.002387	-1.174818	194.459770
244	-0.543287	179.836854	0.000000	-1.142657	193.328854

Table 18: Coefficients of a linear parameterization of the product kinetic energy and the quadratic coefficients of the  $Q(E_n)$  parameterization for the Americium isotopes ( $Z = 95$ ).

Curium ( $_{96}\text{Cm}$ )					
Isotope	Product Kinetic Energy		$Q(E_n)$		
	$b_{\text{TKE}}$	$c_{\text{TKE}}$ (MeV)	$a_Q$ (MeV $^{-1}$ )	$b_Q$	$c_Q$ (MeV)
240	-0.633307	184.208030	0.011040	-1.337777	198.682030
241	-0.632400	183.944134	0.007316	-1.250670	198.592134
242	-0.631501	183.682722	0.011400	-1.346271	198.332722
243	-0.634246	184.481180	0.005492	-1.381016	199.534180
244	-0.633359	184.223119	0.010830	-1.410329	198.275119
245	-0.632480	183.967422	0.005426	-1.387650	198.900422
246	-0.631609	183.714045	0.009390	-1.390179	197.602045
247	-0.633805	184.352758	0.008595	-1.227275	199.517758
248	-0.632945	184.102692	0.013550	-1.366115	198.346692
249	-0.632093	183.854836	0.008907	-1.237463	197.927836
250	-0.631248	183.609152	0.006831	-1.208118	197.531152

Table 19: Coefficients of a linear parameterization of the product kinetic energy and the quadratic coefficients of the  $Q(E_n)$  parameterization for the Curium isotopes ( $Z = 96$ ).

Berkelium ( $_{96}\text{Bk}$ )					
Isotope	Product Kinetic Energy		$Q(E_n)$		
	$b_{\text{TKE}}$	$c_{\text{TKE}}$ (MeV)	$a_Q$ (MeV $^{-1}$ )	$b_Q$	$c_Q$ (MeV)
245	-0.722507	187.420815	0.009615	-1.341277	202.579815
246	-0.721506	187.160975	0.005445	-1.228176	202.383975
247	-0.724256	187.874420	0.008129	-1.280726	202.654420
248	-0.723267	187.617927	0.006656	-1.226737	202.711928
249	-0.722287	187.363720	0.010130	-1.303257	201.831720
250	-0.721316	187.111759	0.008308	-1.283986	201.939760

Table 20: Coefficients of a linear parameterization of the product kinetic energy and the quadratic coefficients of the  $Q(E_n)$  parameterization for the Berkelium isotopes ( $Z = 97$ ).

Californium ( $_{98}\text{Cf}$ )					
Isotope	Product Kinetic Energy		$Q(E_n)$		
	$b_{\text{TKE}}$	$c_{\text{TKE}}$ (MeV)	$a_Q$ (MeV $^{-1}$ )	$b_Q$	$c_Q$ (MeV)
246	-0.814296	190.612254	0.009000	-1.365066	206.461254
248	-0.816539	191.137366	0.010700	-1.411909	206.747367
249	-0.815425	190.876713	0.007067	-1.323895	207.253714
250	-0.814322	190.618383	0.007397	-1.299392	205.793382
251	-0.817010	191.247740	0.010790	-1.354680	207.603739
252	-0.815921	190.992752	0.007184	-1.278611	206.061652
253	-0.814841	190.739978	0.018650	-1.558311	206.137978

Table 21: Coefficients of a linear parameterization of the product kinetic energy and the quadratic coefficients of the  $Q(E_n)$  parameterization for the Californium isotopes ( $Z = 98$ ).

Increasing  $Z$  with fixed  $d_{LH}$  causes  $c_{\text{TKE}}$  to increase with  $ZA$ . One might assume that since fission is more symmetric ( $Z_L \approx Z_H$ ,  $A_L \approx A_H$ ) at higher energies, the average total fission product kinetic energy would increase slightly with  $E_n$  rather than decrease, as implied by the negative slope,  $b_{\text{TKE}}$ . However measurements of fragment kinetic energy as a function of  $A_H$  at fixed  $E_n$  [6, 7] show that the product kinetic energy as a function of mass is a minimum for near symmetric fission. This is a general feature of fission product kinetic energy that has been observed a number of times [6, 7, 8]. It is a result of several effects. The maximum kinetic energy occurs for values of  $A$  where the proton and/or neutron shell is closed ( $Z = 50$ ,  $N = 82$ ). The  $A$  values corresponding to the closed shells are away from the region of symmetric fission. Instead there is a dip in the kinetic energy at symmetric fragment mass thought to be due to the greater deformation of the pre-fragments at the symmetry point, leading to a larger  $d_{LH}$ . Indeed, while we have modeled the kinetic energy slope on the change in  $Z$ , we could as well have modeled the decrease in  $\langle T_p^{\text{tot}}(E_n) \rangle$  on increasing  $d_{LH}$  with incident neutron energy.

The resulting coefficients for  $Q(E_n)$  are also shown in Tables 12-21. For lower values of the fissioning  $Z$ , the slope of  $Q(E_n)$  is essentially governed by the subtraction of  $E_n$  while for  $Z > 95$  or so, the decrease in the product kinetic energy with  $E_n$  is also nearly linear in  $E_n$  so that the overall  $Q(E_n)$  slope is decreasing nearly as  $2E_n$ . The  $Q$  values for all isotopes are shown in Figs. 3-12. These values are tabulated in ENDL2008 in files with **C=15** and **I=12**, a new **I** number for fission. Since  $b_{\text{TKE}}$  and  $b_\gamma$  are nearly independent of  $A$  and only  $a_n \neq 0$ , the difference in the energy dependence of the  $Q$  values for the isotopes of a given  $Z$  comes almost exclusively from  $b_n$ . The isotopes with the weakest energy dependence of  $Q$ , *e.g.*  $^{229}\text{Th}$  and  $^{243}\text{Pu}$ , have the largest  $b_n$  for  $Z = 91$  and  $94$  respectively. The change in  $Q$  with  $E_n$  for  $0 < E_n < 20$  MeV is on the order of 10% or less.

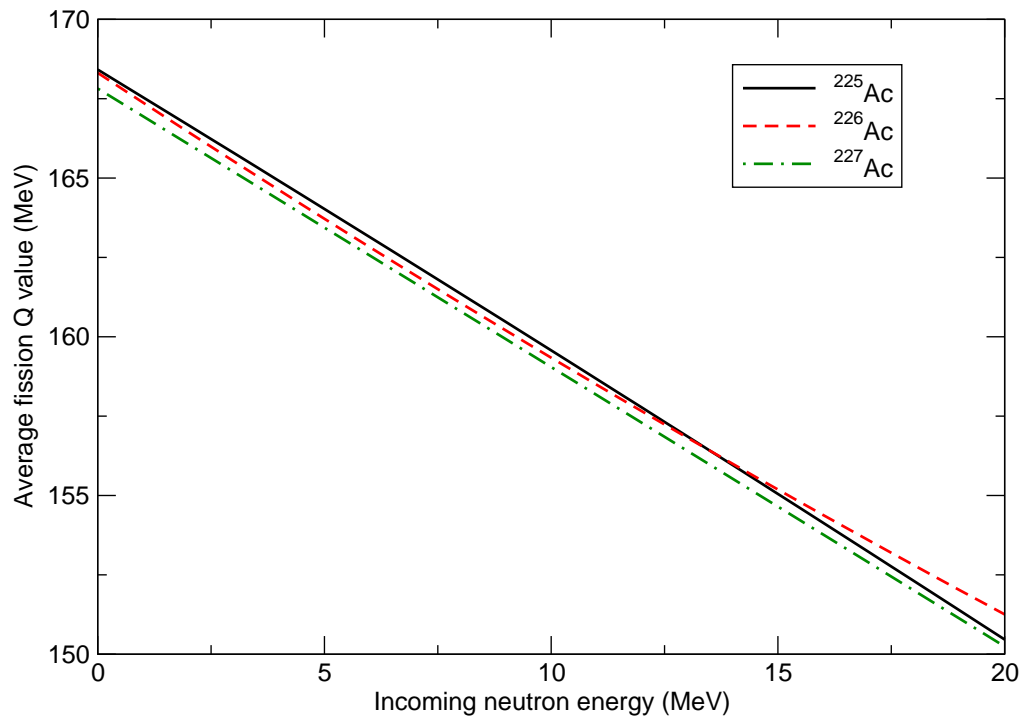


Figure 3: The energy dependence of the fission  $Q$  value for the Actinium isotopes ( $Z = 89$ ).

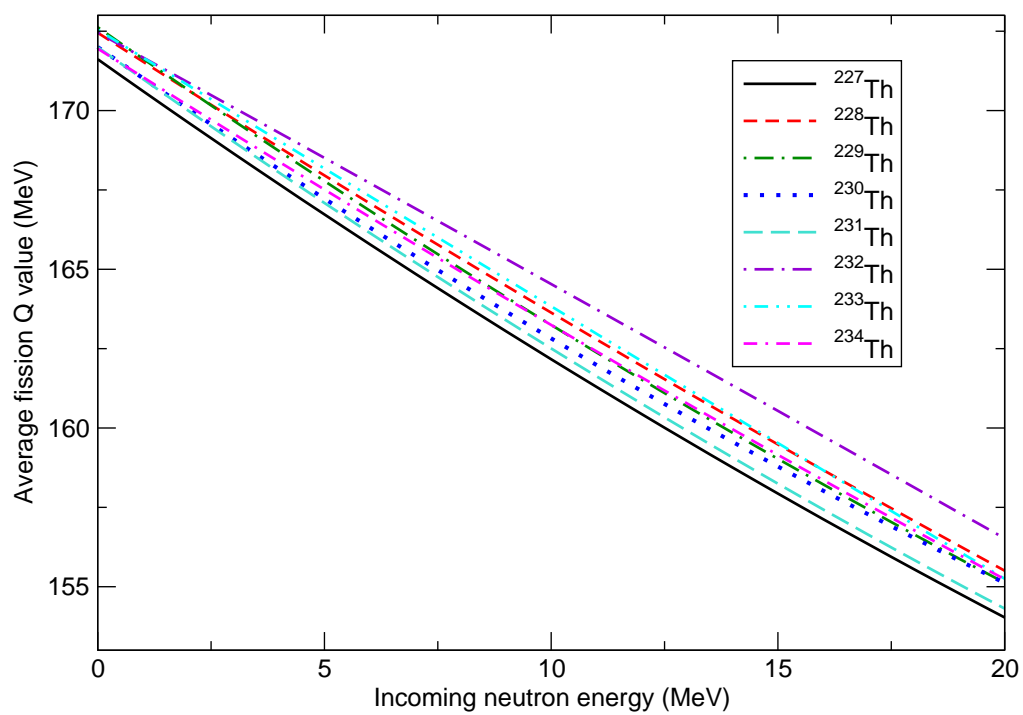


Figure 4: The energy dependence of the fission  $Q$  value for the Thorium isotopes ( $Z = 90$ ).

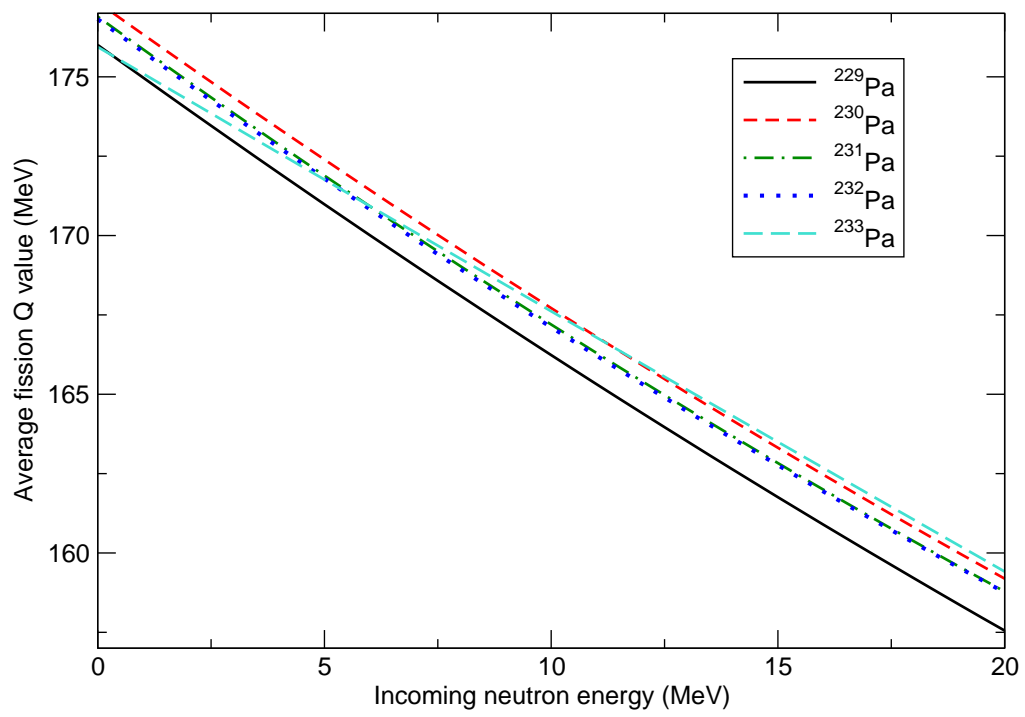


Figure 5: The energy dependence of the fission  $Q$  value for the Protactinium isotopes ( $Z = 91$ ).

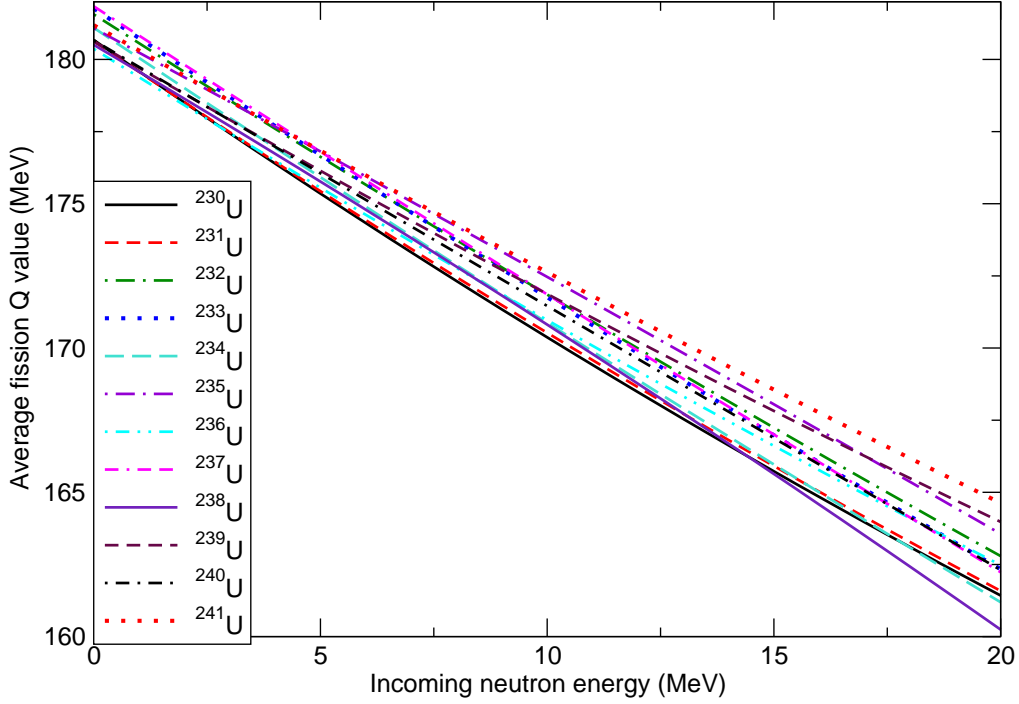


Figure 6: The energy dependence of the fission  $Q$  value for the Uranium isotopes ( $Z = 92$ ).

Figure 13 compares our general  $Q(E_n)$  relative to the parameterization by Madland [1, 3]. At  $E_n \approx 0$  the difference is less than 1% and increases slightly with energy. The differences between the various model components are shown in Fig. 14. The two results for  $\langle E_{\text{neut}}^{\text{tot}}(E_n) \rangle$  are nearly identical at  $E_n < 15$  MeV, only deviating slightly at higher energies. The differences in average product kinetic energy as a function of  $E_n$  are also rather small. Madland uses a quadratic parameterization of the  $^{238}\text{U}$  kinetic energy, causing the upward curvature at large  $E_n$ . There is about 1 MeV difference in the kinetic energy for  $^{239}\text{Pu}$  over the entire energy range. Thus neither the product kinetic energy nor the energy given to the prompt neutron emission will cause a large deviation between the  $Q(E_n)$  parameterizations. The difference observed in the two calculations with increasing  $E_n$  is due to the prompt gamma parameterizations. Madland's values, neither in ENDF/B-VII [9] nor in ENDL99, typically exhibit a slower energy dependence than our fits to the ENDL99 I=10 files for these isotopes. Our almost energy independent parameterization of  $^{238}\text{U}$  gives a steeper  $Q(E_n)$  than Ref. [1] where the flattening of  $T_p^{\text{tot}}$  combined with the increase of  $E_\gamma^{\text{tot}}$  act to make Madland's  $Q(E_n)$  decrease more slowly than our model. At 20 MeV, the difference is



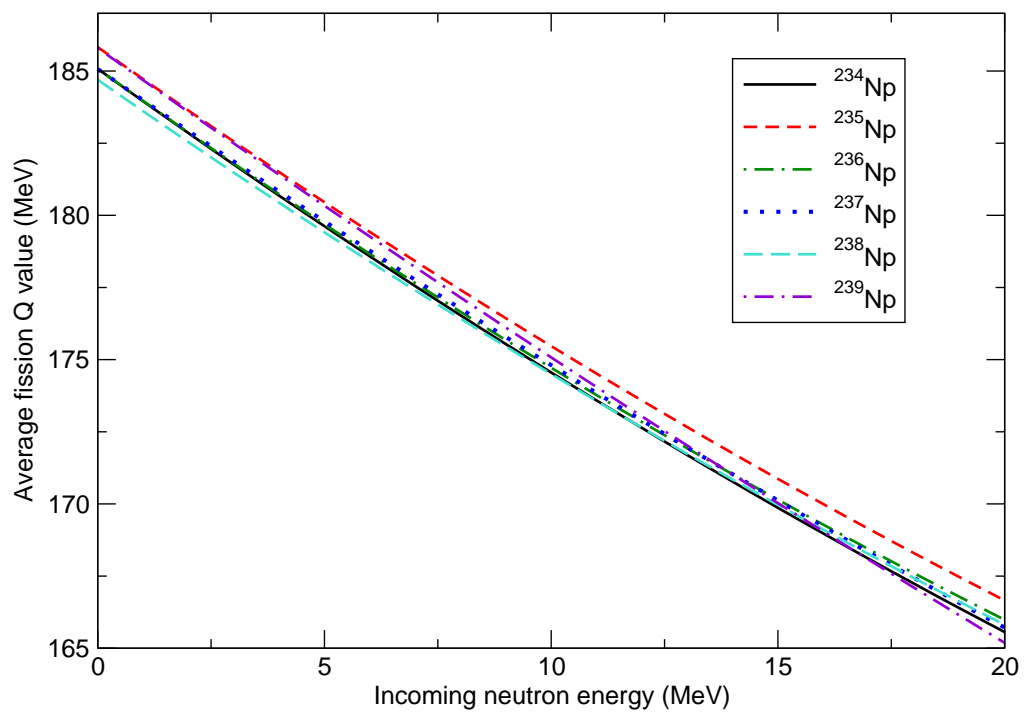


Figure 7: The energy dependence of the fission  $Q$  value for the Neptunium isotopes ( $Z = 93$ ).

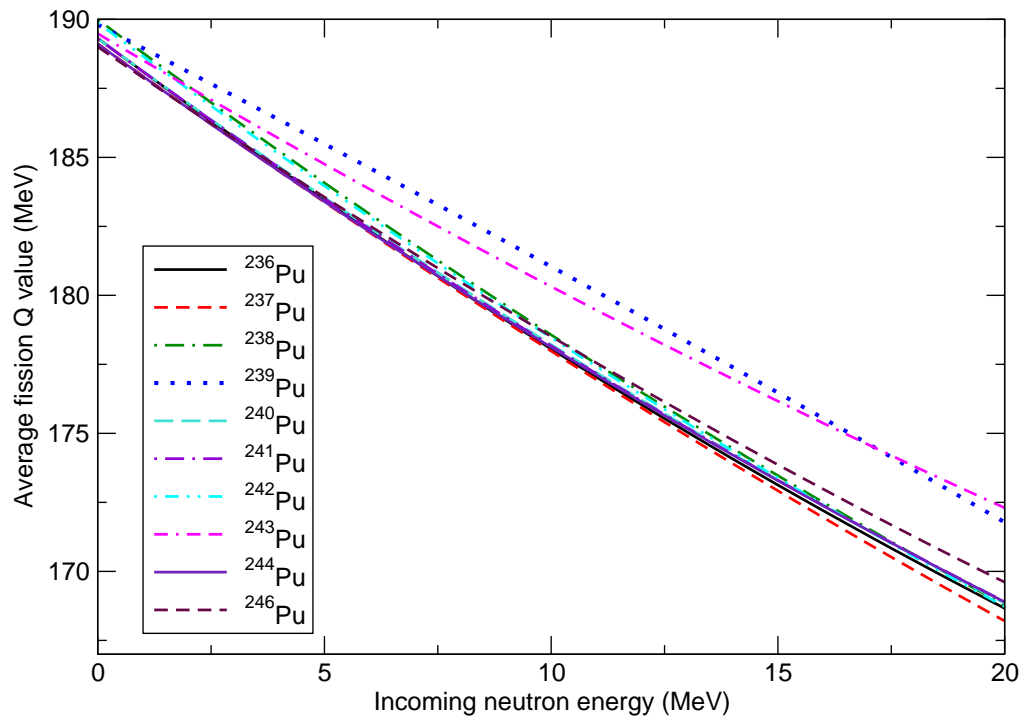


Figure 8: The energy dependence of the fission  $Q$  value for the Plutonium isotopes ( $Z = 94$ ).

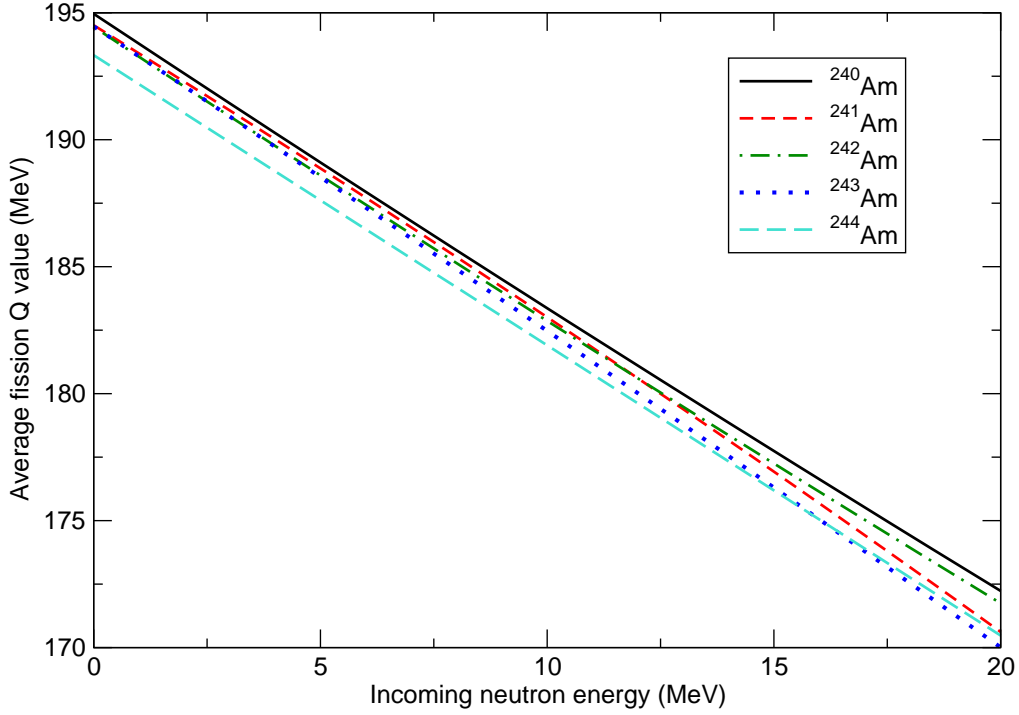


Figure 9: The energy dependence of the fission  $Q$  value for the Americium isotopes ( $Z = 95$ ).

about 3%. The two results for  $^{235}\text{U}$  are small and remain so throughout the range of incident neutron energy. The largest difference is in the  $^{239}\text{Pu}$  results. The change in slope of the two calculations can be attributed to the stronger energy dependence of  $E_{\gamma}^{\text{tot}}$  in our parameterization. Without further clarification of the prompt gamma emission energy, a discrepancy of about 3% remains.

We have generalized Madland's parameterization of the fission energy release and energy deposition [1] to obtain the fission  $Q$  value for neutron-induced fission of all the actinides in the ENDL2008 release. The  $Q$  value decreases  $\approx 10\%$  for all actinides over the range from thermal neutron energies to  $E_n = 20$  MeV.

**Acknowledgements** I would like to thank D. A. Brown for many useful discussions.

## References

- [1] D. Madland, Nucl. Phys. A **772** (2006) 113.

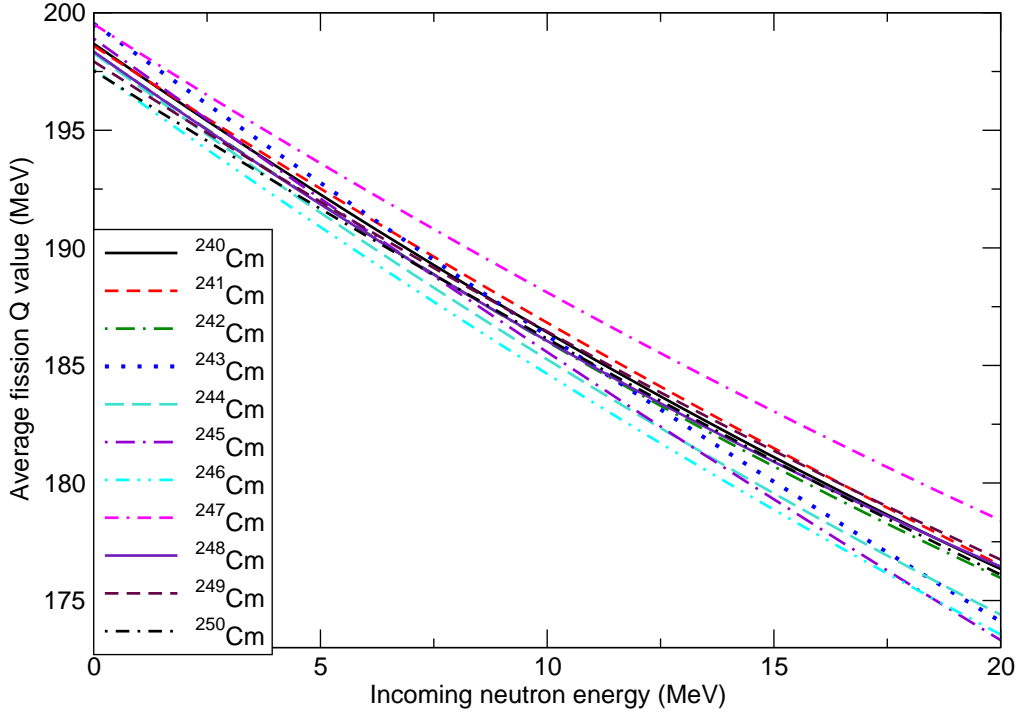


Figure 10: The energy dependence of the fission  $Q$  value for the Curium isotopes ( $Z = 96$ ).

- [2] G. W. Hedstrom, L. J. Cox and S. T. Perkins, UCRL-ID-127438 (1997).
- [3] R. Vogt, B. Beck, D. A. Brown, F. Daffin and J. Hedstrom, UCRL-TR-234617.
- [4] B. Beck, G. W. Hedstrom, T. S. Hill, A. A. Marchetti and D. P. McNabb, UCRL-TM-218475 (2006).
- [5] K.-H. Schmidt, S. Steinhäuser, C. Böckstiegel, A. Grewe, A. Heinz, A. R. Junghans, J. Benlliure, H.-G. Clerc, M. deJong, J. Müller, M. Pfützner and B. Voss, Nucl. Phys. A **665** (2000) 221.
- [6] H. W. Schmitt, J. H. Neiler and F. J. Walter, Phys. Rev. **141** (1966) 1146.
- [7] J. N. Neiler, F. J. Walter and H. W. Schmitt, Phys. Rev. **149** (1966) 894.
- [8] J. C. D. Milton and J. S. Fraser, Can. J. Phys. **40** (1962) 1626; Phys. Rev. Lett. **7** (1961) 67.

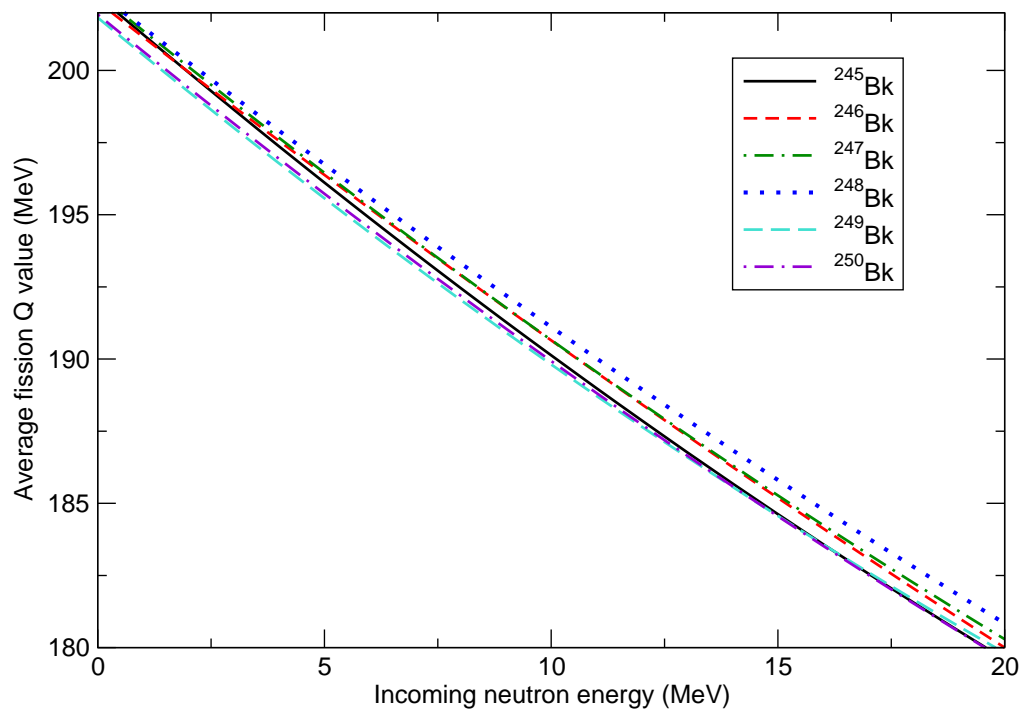


Figure 11: The energy dependence of the fission  $Q$  value for the Berkelium isotopes ( $Z = 97$ ).

[9] M. B. Chadwick *et al.*, Nuclear Data Sheets **107** (2006) 2931.

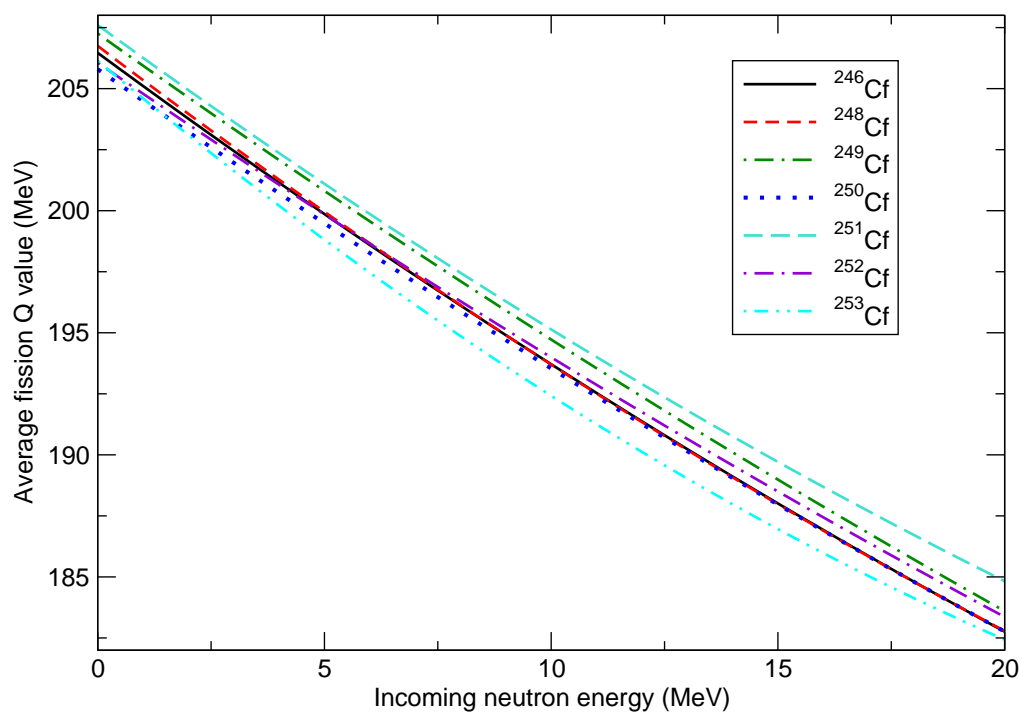


Figure 12: The energy dependence of the fission  $Q$  value for the Californium isotopes ( $Z = 98$ ).

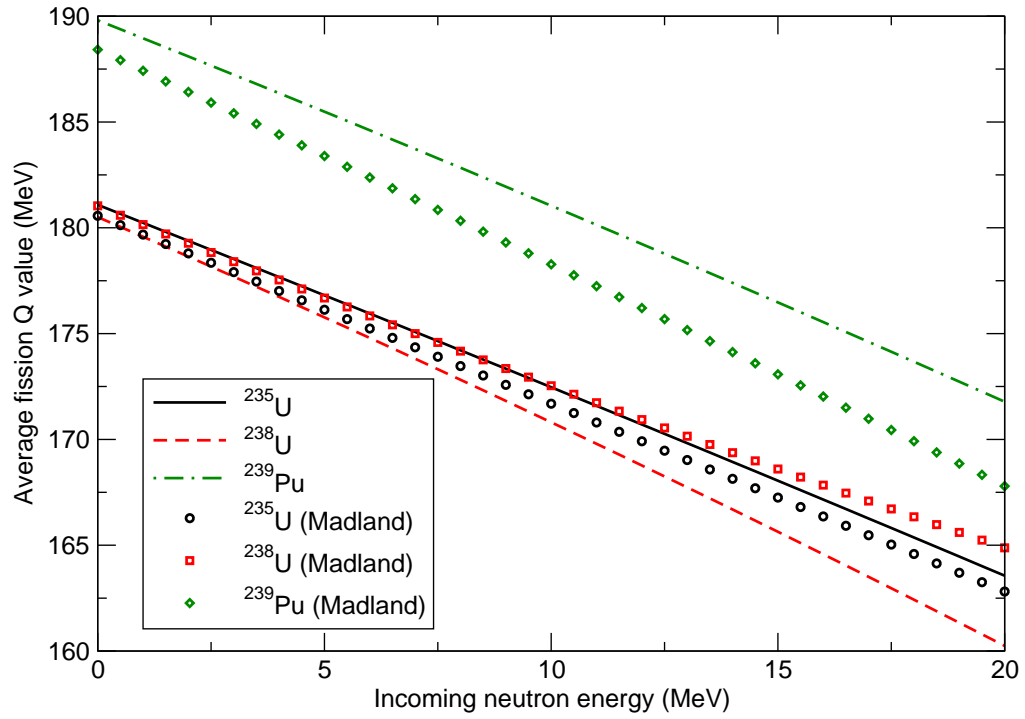


Figure 13: Comparison of  $Q(E_n)$  from this paper (lines) and Refs. [1, 3] (symbols). Results are shown for  $^{235}\text{U}$  (black solid line, circles),  $^{238}\text{U}$  (red dashed line, squares), and  $^{239}\text{Pu}$  (green dot-dashed line, diamonds).

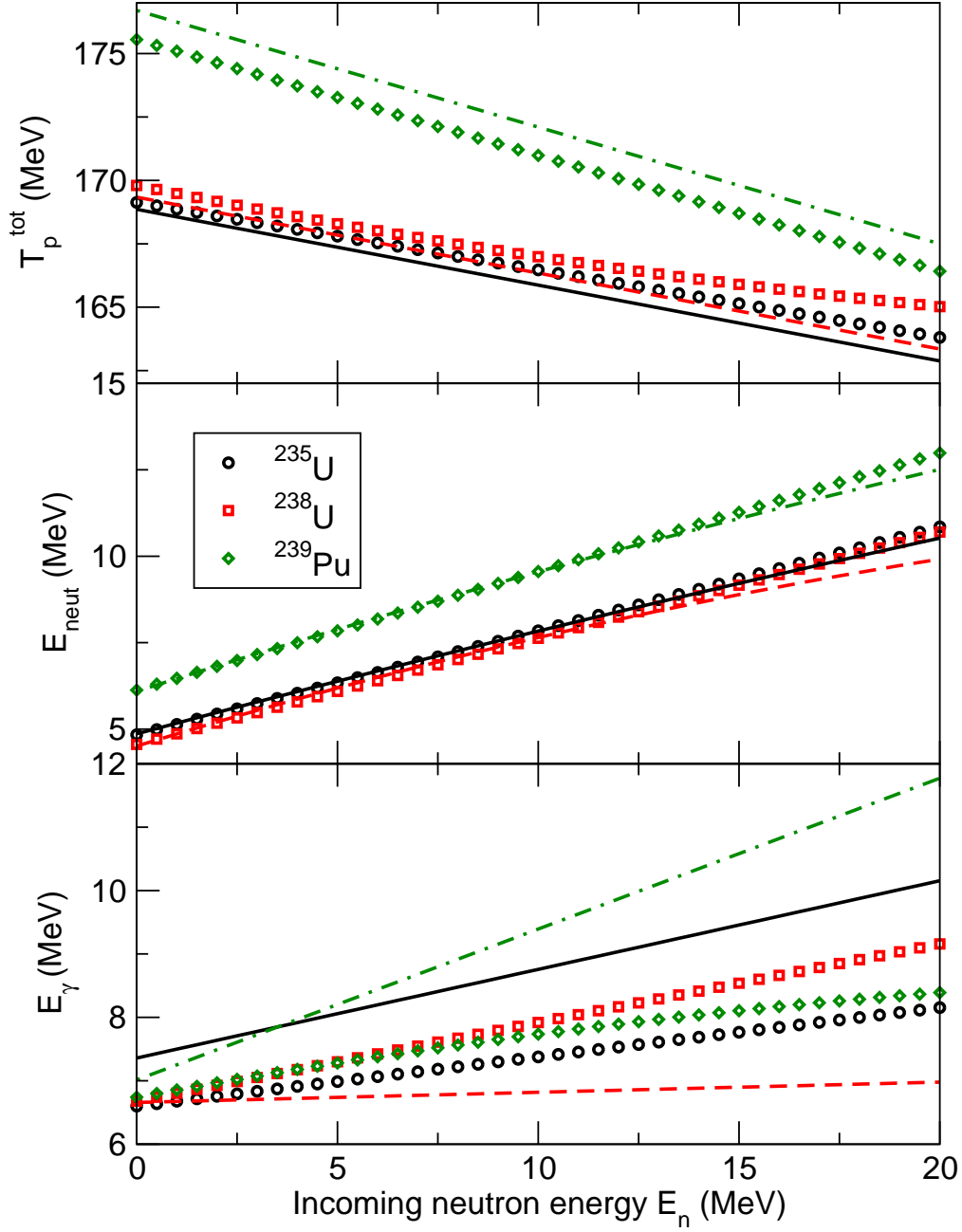


Figure 14: Comparison of the kinetic energy (top), neutron emission energy (center) and gamma emission energy (bottom) from this paper (lines) and Refs. [1, 3] (symbols). Results are shown for  $^{235}\text{U}$  (black solid line, circles),  $^{238}\text{U}$  (red dashed line, squares), and  $^{239}\text{Pu}$  (green dot-dashed line, diamonds).